Vol. 75, No. 6

Differential Interaction of Dendritic Cells with *Rickettsia conorii*: Impact on Host Susceptibility to Murine Spotted Fever Rickettsiosis[▽]

Rong Fang,[1] Nahed Ismail,[1] Lynn Soong,[1,2] Vsevolod L. Popov,[1] Ted Whitworth,[1]
Donald H. Bouyer,[1] and David H. Walker[1]*

Department of Pathology[1] and Department of Microbiology and Immunology,[2] University of Texas Medical Branch, Galveston, Texas

Spotted fever group rickettsioses are emerging and reemerging infectious diseases, some of which are life-threatening. In order to understand how dendritic cells (DCs) contribute to the host resistance or susceptibility to rickettsial diseases, we first characterized the in vitro interaction of rickettsiae with bone marrow-derived DCs (BMDCs) from resistant C57BL/6 (B6) and susceptible C3H/HeN (C3H) mice. In contrast to the exclusively cytosolic localization within endothelial cells, rickettsiae efficiently entered and localized in both phagosomes and cytosol of BMDCs from both mouse strains. *Rickettsia conorii*-infected BMDCs from resistant mice harbored higher bacterial loads compared to C3H mice. *R. conorii* infection induced maturation of BMDCs from both mouse strains as judged by upregulated expression of classical major histocompatibility complex (MHC) and costimulatory molecules. Compared to C3H counterparts, B6 BMDCs exhibited higher expression levels of MHC class II and higher interleukin-12 (IL-12) p40 production upon rickettsial infection and were more potent in priming naïve CD4$^+$ T cells to produce gamma interferon. In vitro DC infection and T-cell priming studies suggested a delayed CD4$^+$ T-cell activation and suppressed Th1/Th2 cell development in C3H mice. The suppressive CD4$^+$ T-cell responses seen in C3H mice were associated with a high frequency of Foxp3$^+$ T regulatory cells promoted by syngeneic *R. conorii*-infected BMDCs in the presence of IL-2. These data suggest that rickettsiae can target DCs to stimulate a protective type 1 response in resistant hosts but suppressive adaptive immunity in susceptible hosts.

Rickettsiae are gram-negative, obligately intracellular bacteria that can cause human illness with fatal outcome in certain cases. *Rickettsia conorii* is the etiologic agent of boutonneuse fever and is the most geographically dispersed spotted fever group rickettsial species (53). Endothelial cells are the major target of *Rickettsia*. However, rickettsiae can also invade other cells, such as macrophages. *R. conorii* is transmitted to humans by the brown dog tick *Rhipicephalus sanguineus*, causing disseminated intraendothelial cell infection that manifests typically as fever, rash, and vasculitis. This disease varies in severity and is fatal in 1 to 5% of hospitalized cases. Currently, fatal and severe cases of Mediterranean spotted fever are occurring in areas of endemicity (1, 7).

Protective immunity against rickettsial infection is characterized by substantial production of gamma interferon (IFN-γ) and generation of cytotoxic T lymphocytes (9, 46). Natural killer (NK) cells and macrophages are involved in the innate immune response against *Rickettsia* (48). Human cells, including endothelial cells, hepatocytes, and macrophages, are capable of controlling intracellular *R. conorii* organisms by one or a combination of three mechanisms, including nitric oxide synthesis, hydrogen peroxide production, and tryptophan degradation (11). Despite these findings, there is still a large gap in our understanding regarding the initial interaction between tick-transmitted rickettsiae and host immune cells at the site of inoculation, the dermis of the skin, and the effect of this inter-

action on the acquired immune response in secondary lymphoid organs (21, 48). The fate and severity of rickettsial infection could well be decided at an early point after the bacterial inoculation by an infected arthropod. Until now, the early events in innate immunity to rickettsiae have been poorly understood. Furthermore, the role of CD4$^+$ T cells in host defense against rickettsial infection still remains unclear.

Experimental studies in animal models of *R. conorii* infection have been the basis of our previous analyses of immunity to rickettsiae. Among different mouse strains, C57BL/6 (B6) mice are highly resistant while C3H/HeN (C3H) mice are highly susceptible to lethal infection with *R. conorii* (46, 47). However, the critical immune effectors that determine the resistance or susceptibility to fatal disease are still under investigation.

Dendritic cells (DCs) are the most potent antigen-presenting cells that link the innate and adaptive immune responses and are critical to triggering specific immunity. DCs are critical factors in the host defense system against many pathogens due to their capability to capture antigens, migrate to lymph nodes, and effectively activate naïve CD4$^+$ and CD8$^+$ T lymphocytes (20, 51). Earlier studies demonstrated that DCs play an important role in regulation of host responses against intracellular bacteria, such as *Salmonella* and *Listeria* (4, 50). However, until now the interactions between rickettsiae and DCs have not been reported.

In this study, we investigated the differential interactions of bone marrow-derived DCs (BMDCs) from mice that are highly susceptible or resistant to *R. conorii*. We sought to determine whether the initial interactions of *R. conorii* and BMDCs could account for the susceptibility or resistance to spotted fever

---

* Corresponding author. Mailing address: Center for Biodefense and Emerging Infectious Diseases, 301 University Blvd., Galveston, TX 77555-0609. Phone: (409) 772-3989. Fax: (409) 772-1850. E-mail: dwalker@utmb.edu.

rickettsiosis. Our results showed differential interactions of rickettsiae with BMDCs in C3H mice from those in B6 mice in vitro, including capability of antigen capture, cytokine production, and maturation status, which promote differential naïve CD4^{+} T-cell activation and polarization. Our data provided the first evidence suggesting that priming of CD4^{+} Th1/Th2 responses and induction of regulatory T cells by *Rickettsia*-infected DCs might be the critical factors in determining resistance or susceptibility to rickettsial diseases.

MATERIALS AND METHODS

***Rickettsia* culture and preparation.** *R. conorii* (Malish 7 strain) was obtained from the American Type Culture Collection (ATCC VR 613). Rickettsiae were propagated in Vero cells and purified by renografin density centrifugation as described previously (17). Purified viable rickettsiae were suspended in sucrose-phosphate-glutamate buffer (0.218 M sucrose, 3.8 mM KH_2PO_4, 7.2 mM K_2HPO_4, 4.9 mM monosodium glutamic acid, pH 7.0; 1 ml per 10 original 150-cm^2 flasks). The concentration of rickettsiae was determined by plaque assay and quantitative real-time PCR as described below (12). The rickettsial stock was stored at $-80°C$ at a concentration of 2×10^8 PFU/ml until use.

Animals and rickettsial infection. Age- and sex-matched C3H and B6 mice were the sources of in vitro generation of BMDCs. Specific-pathogen-free mice were purchased from Harlan Laboratories (Indianapolis, IN) and were housed in a biosafety level 3 facility at the University of Texas Medical Branch, Galveston. All experiments and procedures were approved by the University of Texas Medical Branch Animal Care and Use Committee, and mice were used according to the guidelines in the *Guide for the Care and Use of Laboratory Animals*. C3H and B6 mice (six mice per group, including three infected mice and three negative controls) were infected intravenously as described previously with 5×10^5 PFU of *R. conorii* (10 50% lethal doses [LD_{50}] for C3H mice) (47). Negative controls were inoculated with 100 μl of SPG buffer alone. Mice were monitored daily for signs of illness, including loss of appetite, ruffled fur, weight loss, and decreased activity.

Generation of DCs from bone marrow. Phenotypically stable immature DCs (CD11c$^+$) were isolated from bone marrow of B6 and C3H mice. The protocol for generating BMDCs was performed as originally described (19, 31). Briefly, a single-cell suspension from bone marrow was prepared from the mouse femurs and adjusted to 2×10^6 cells per 10 ml of complete Iscove's modification of Dulbecco's modified Eagle's medium containing 10% fetal bovine serum, 1 mM sodium pyruvate, 50 μM 2-mercaptoethanol, 100 μg/ml streptomycin sulfate, and 100 U/ml penicillin). DC culture medium was supplemented with 20 ng/ml recombinant granulocyte-macrophage colony-stimulating factor (GM-CSF; eBioscience, San Diego, CA) or with 2% culture supernatants of J558L cells that were stably transfected with the murine *gm-csf* gene (39). At day 3, 6 ml of fresh GM-CSF-containing medium was added, and 10 ml of the culture medium was replaced with fresh GM-CSF-containing medium at day 6. On day 8, cultures were examined by fluorescence-activated cell sorter analysis and were used if they contained ≥70 to 75% CD11c$^+$ cells.

In vitro infection of BMDCs with *R. conorii*. On day 8 of culture, BMDCs were collected and 10^6 cells/ml were seeded into 24-well culture plates with complete medium without antibiotics. *R. conorii* was inoculated into each well at a multiplicity of infection (MOI) of 5:1. To synchronize bacterial internalization, rickettsiae were first centrifuged onto the cells at $560 \times g$ for 5 min. At 4 h, noninternalized bacteria were removed by washing the cell culture with phosphate-buffered saline several times. Cells were continually cultivated at 37°C with 5% CO_2 in fresh complete medium. Uninfected BMDCs were used as negative controls. At different time points, supernatants and infected or uninfected BMDCs were collected for further analysis. Aliquots of cells were prepared in a cytospin and stained using Diff-Quik (Fisher Scientific, Pittsburgh, PA) to estimate the level of infection. As positive controls, some wells containing BMDCs were stimulated with 100 ng or 2 μg/ml of *Escherichia coli* lipopolysaccharide (LPS; Sigma, St. Louis, MO).

Electron microscopic analysis of *R. conorii*-infected BMDCs. For examination of infected BMDCs by electron microscopy, BMDCs were harvested at 24 h of infection and immersed in Ito's fixative (1.25% formaldehyde, 2.5% glutaraldehyde, 0.03% $CaCl_2$, and 0.03% trinitrophenol in 0.05 M cacodylate buffer, pH 7.3) at room temperature for 1 h and then overnight at 4°C. After washing, samples were processed further as described previously (22). Ultrathin sections were cut on a Sorvall MT-6000 ultramicrotome (RMC, Tucson, AZ) and examined in a Philips 201 transmission electron microscope (Philips Electron Optics,

Eindhoven, The Netherlands) at 60 kV. As a control, the subcellular rickettsial localization within BMDCs was compared to that detected in endothelial cells (the main target cells for *Rickettsia*) prepared and infected with rickettsiae as described previously (13, 39). For each sample, approximately 100 cells were examined.

Quantification of bacterial loads by quantitative real-time PCR. To determine the number of intracellular rickettsiae following in vitro infection, *R. conorii*-infected BMDCs were collected at different time intervals postinfection as described above, and DNA was extracted from these cells using QIAGEN DNA extraction kits (Valencia, CA).

Quantitative real-time PCR was performed using the iCycler from Bio-Rad (Hercules, CA). The rickettsial load was determined by real-time PCR with Taqman probes for the *Rickettsia*-specific gene *ompB* as described in our previous studies (44). The *R. conorii ompB* probe was labeled with 6-carboxyfluorescein and Black Hole Quencher 1, and the probe for *gapdh* was labeled with 6-carboxytetramethylrhodamine and Black Hole Quencher 2 (Biosearch Technologies, Novato, CA). Two-step cycle parameters (95°C and 60°C) were used, and the primers and probes were described previously (*gapdh* forward, CAAC TACATGGTCTACATGTTC; *gapdh* reverse, CTCGCTCCTGGAAGATG; *gapdh* probe, CGGCACAGTCAAGGCCGAGAATGGGAAGC; *ompB* forward, ACACATGCTGCCGAGTTACG; *ompB* reverse, AATTGTAGCACTA CCGTCTAAGGT; *ompB* probe, CGGCTGCAAGAGCACCGCCAACAA). The results were normalized to *gapdh* in the same sample and expressed as copy number per 10^4 copies of *gapdh*.

Flow cytometry. Flow cytometry was performed to characterize the populations of immune lymphocytes or BMDCs stimulated by antigens of *R. conorii*. To block nonspecific antibody binding, normal mouse immunoglobulin G (IgG), hamster IgG, rat IgG (Pierce, Rockford, IL), and anti-mouse FcγIII/II receptors (clone 2.4G2; BD Bioscience, San Diego, CA) were used in BMDC staining. The following fluorescein isothiocyanate-, phycoerythrin (PE)-, peridinin chlorophyll *a* protein-, and allophycocyanin-conjugated antibodies (Abs) were purchased from BD Bioscience unless indicated otherwise: anti-CD3 (145-2C11), anti-CD11c (HL3), anti-CD4 (RM4-5), anti-CD25 (PC 61), anti-CD11b (M1/70), anti-*I-A^d/E^d* (M5/114.15.2), anti-*H2D^b* (KH95), anti-CD40 (3/23), anti-CD80 (16-10A1), anti-CD86 (GL1), anti-CD69 (H1.2F3), anti-IFN-γ (XMG1.2), anti-interleukin-4 (IL-4; 11B11), and anti-IL-10 (JES5-16E3). Isotype control Abs included fluorescein isothiocyanate-, PE-, peridinin chlorophyll *a* protein-, and allophycocyanin-conjugated hamster IgG1 (A19-3), rat IgG1 (R3-34), rat IgG2a (R35-95), mouse IgG2a (X39), mouse IgG2b (MPC-11), mouse IgG1 (X40), and rat IgG2b (A95-1), and PE-conjugated anti-*H2D^k* (15-5-5) was purchased from Biolegend (San Diego, CA). Staining with anti-Foxp3-PE-conjugated Ab (FJK-16S) was performed according to the manufacturer's protocol (eBioscience). Stained cells were analyzed on a FACScan (BD Biosciences, Franklin Lakes, NJ). For characterization of BMDCs, at least 10,000 CD11c$^+$ events were collected. For characterization of T cells, at least 20,000 events were collected. Data were analyzed with FlowJo software (TreeStar, San Carlos, CA).

Cytokine assays for rickettsiae-exposed BMDCs. BMDCs were inoculated with purified *R. conorii* in 24-well plates. Supernatants were harvested at 18 h and 24 h following infection and stored at $-70°C$ until examined. IL-4, IL-12p40, IL-12p70, and IFN-γ were measured by using Quantikine enzyme-linked immunosorbent assay (ELISA) kits (R&D Systems, Minneapolis, MN). The sensitivities of ELISA for cytokine measurements were as follows: 2 pg/ml for IL-4, 4 pg/ml for IL-12p40, 2.5 pg/ml for IL-12p70, and 20 pg/ml for IFN-γ.

Nitric oxide determination from *Rickettsia*-exposed BMDCs. The levels of nitric oxide (NO) produced by *Rickettsia*-exposed BMDCs were measured by using a Griess assay kit (Promega, Madison, WI). Briefly, culture supernatants were added to 96-well microplates at 50 μl in each well. Following the addition of Griess reagent (50 μl/well), the plates were incubated at room temperature for 10 min. The absorbance was determined using a microplate reader at 570 nm. The concentrations of NO_2^- were calculated against the standard curve generated based on known concentrations of $NaNO_2$. In some experiments, BMDCs were infected with rickettsiae in the presence of 1 mM N^G-monomethyl-L-arginine (L-NMMA; Sigma, St. Louis, MO), an inhibitor for inducible nitric oxide synthase.

Activation and differentiation of naïve syngeneic T cells stimulated in vitro by *R. conorii*-infected BMDCs. Syngeneic CD4$^+$ T cells from naïve C3H and B6 mice were purified with negative selection kits (Miltenyi Biotec, California). The purity of obtained CD4$^+$ T cells was 93 to 96% as determined by flow cytometry. Day 8 BMDCs from C3H and B6 mice were infected with *R. conorii* for 6 h or 24 h, washed extensively, and cocultured with purified CD4$^+$ T cells (total, 8×10^5 cells/well) at a DC/T-cell ratio of 1:4 or 1:10 in 96-well plates. As negative and positive controls, aliquots of the same naïve syngeneic T cells were cocultured with uninfected BMDCs or LPS-treated BMDCs, respectively. At 48 h or 72 h of
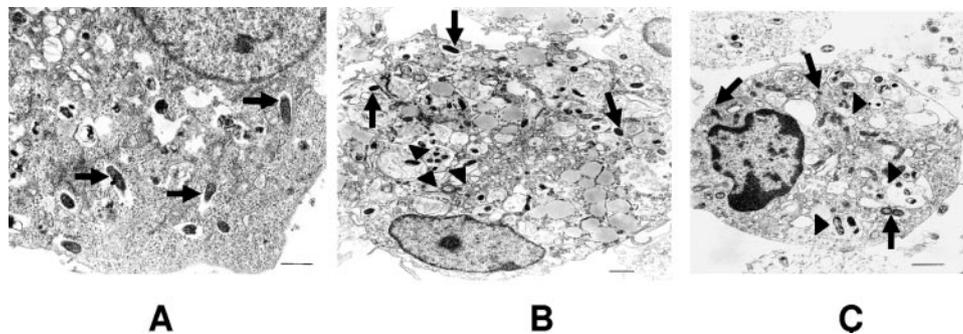
FIG. 1. Ultrastructure of *R. conorii*-infected BMDCs and endothelial cells. Endothelial cells (A) and BMDCs derived from C3H mice (B) and B6 mice (C) were infected with bacteria (MOI of 5) for 24 h and then processed for ultrastructural analysis. (A) Numerous rickettsiae were detected in the cytosol of infected endothelial cells (arrows). (B and C) Bacteria were detected in both the vacuoles (arrowheads) and cytosol (arrows) of BMDCs. Data shown are representative images of three independent experiments with similar results. Bar, 1 μM.

coculture, cells were harvested and stained with CD4, CD3, CD69, and IFN-γ (BD Bioscience). For detection of intracellular cytokines, T cells were continuously cocultured with *R. conorii*-infected BMDCs in the presence of recombinant murine IL-2 (10 ng/ml; BD Bioscience). On day 5, cells were stimulated with phorbol 12-myristate 13-acetate (10 ng/ml) and inomycin (400 ng/ml) for 5 h followed by incubation with Golgi plug or Golgi stop (BD Bioscience) for 6 to 8 h. Finally, cells were harvested and stained for the expression of CD4, CD3, CD25, IFN-γ, IL-4, Foxp3, and IL-10. Cytokine concentrations of IL-4, IL-10, and IFN-γ in culture supernatants were determined by ELISA (R&D Systems). The concentration of *R. conorii*-specific cytokines was determined by subtraction of cytokine concentration in the supernatant of syngeneic T cells cocultured with uninfected BMDCs from that detected in the supernatant of T cells cocultured with *R. conorii*-infected BMDCs.

Statistical analysis. For comparison of mean values of different experimental groups, the two-tailed *t* test was used, and *P* values were calculated using Sigma-Plot software (SPSS, Chicago, IL). A difference in mean values was deemed significant when *P* was <0.05 or highly significant when *P* was <0.01.

RESULTS

Differential susceptibility of different mouse strains to *R. conorii*. Previous studies showed that C3H mice succumb to infection with a high dose of *R. conorii*, while B6 mice are resistant to rickettsial infection (46). To document the differential host susceptibilities to this bacterium, we examined the survival rate in B6 and C3H mice after intravenous infection with *R. conorii* at 5×10^5 PFU, which is 10 LD$_{50}$ for C3H mice (47). As shown previously, C3H mice developed progressive disease, and all mice succumbed to infection on day 6 to 7 postinfection. However, all infected B6 mice survived under the same infection conditions.

***Rickettsia* establishes infection in BMDCs.** To test whether different susceptibilities to *R. conorii* infection in these two mouse strains were due to differential responses at the DC level, we first determined the efficiency of rickettsial infection of BMDCs 24 h after inoculation. Light microscopic examination of cytospin preparations of BMDCs from C3H or B6 mice cultured with *R. conorii* at an MOI of 5:1 showed that BMDCs from both mouse strains ingested rickettsiae, and the rate of infection of BMDCs from both C3H and B6 mice was 100%. To examine rickettsial subcellular localization inside BMDCs, infected BMDCs were processed for electron microscopy. Similar to other reports (13), we observed immediate escape of rickettsiae into the cytosol following entry into their main target cells, endothelial cells (Fig. 1A). Surprisingly, many rickettsiae were localized within cytoplasmic vacuoles (Fig. 1B and

C) in BMDCs from both mouse strains as well as free in the cytosol (Fig. 1B and C). Similar results were observed at 4, 24, 48, and 72 h postinfection (data not shown).

To determine the differences in bacterial uptake, intracellular microbicidal effector mechanisms, and/or rickettsial replication between BMDCs from C3H and B6 mice, infected BMDCs were harvested at different time points, and the quantity of intracellular rickettsiae was determined by quantitative real-time PCR. At 4 h postinfection, immature BMDCs from B6 mice harbored a relatively higher number of bacteria than cells from C3H mice (*P* = 0.09), indicating efficient phagocytosis by BMDCs from both mouse strains and higher bacterial internalization by B6 BMDCs compared to C3H BMDCs (Fig. 2A). At 24 h postinfection, BMDCs from both B6 and C3H mice effectively processed or eliminated intracellular bacteria, as evidenced by reduced quantities of rickettsiae compared to those detected at 4 h postinfection. At 48 h postinfection, BMDCs from both mouse strains supported bacterial replication. Interestingly, although B6 BMDCs possessed a higher rickettsial number than C3H BMDCs at different time intervals, B6 BMDCs exhibited a greater intracellular bactericidal effect than C3H BMDCs as judged by the following: (i) substantial reduction in the number of intracellular rickettsiae at 24 h compared to 4 h postinfection (80% killing in B6 mice versus 40% killing in C3H mice) (Fig. 2B); (ii) less replication of rickettsiae at 48 h compared to 24 h postinfection (11-fold increase in intracellular rickettsiae in B6 mice versus 18-fold increase in C3H mice) (Fig. 2C). Taken together, these data suggest that rickettsiae were effectively internalized by BMDCs from both genetic backgrounds, with greater bacterial internalization and rickettsicidal activities by BMDCs from resistant B6 mice than susceptible C3H mice. Furthermore, the different rickettsial localization within BMDCs compared to endothelial cells could enhance access of rickettsial antigens to the exogenous and endogenous pathways of antigen presentation to CD4$^+$ and CD8$^+$ T cells.

Differential NO induction by *R. conorii*-infected BMDCs from different mouse strains. We have previously demonstrated that production of NO by host target cells such as endothelial cells and hepatocytes stimulated by IFN-γ and tumor necrosis factor alpha is one of the intracellular rickettsicidal mechanisms that are critical for bacterial elimina-
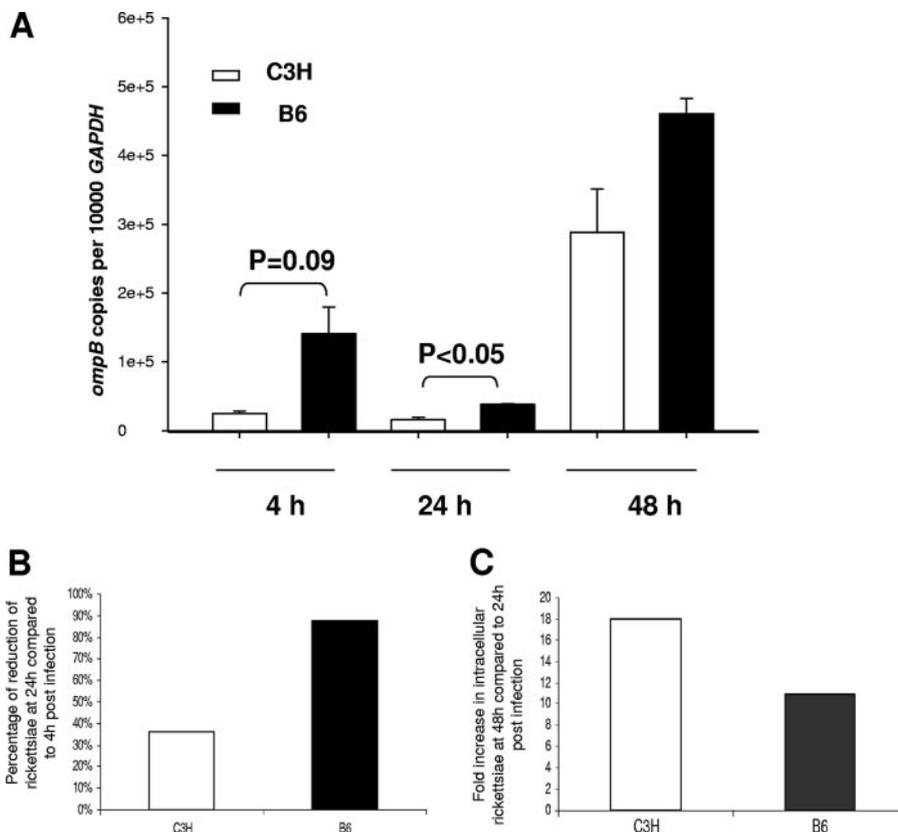
FIG. 2. Quantification of intracellular rickettsiae in *R. conorii*-infected BMDCs. BMDCs derived from C3H mice and B6 mice were infected with bacteria (MOI of 5). (A) At 4 h postinfection, extracellular bacteria were removed, and the quantities of intracellular bacteria were determined at 4 h, 24 h, and 48 h postinfection by quantitative real-time PCR. Data are presented as means ± standard deviations of three replicates in each group. (B) The percentages of killed or processed bacteria from 4 h to 24 h postinfection were calculated using the average quantity of rickettsiae at these two time points. Compared to 24 h postinfection, the average quantity of intracellular bacteria at 48 h in BMDCs from the two mouse strains had increased to a different degree. Data shown are representative of results from three independent experiments.

tion (9–11). To determine whether NO plays a role in innate defense against *Rickettsia* infection in DCs, we measured NO production in the supernatant of *R. conorii*-infected BMDC cultures in the presence or absence of the inducible nitric oxide synthase inhibitor L-NMMA. Uninfected BMDCs from both mouse strains produced a low concentration of NO (Fig. 3). Following rickettsial infection, BMDCs from both mouse strains produced increased quantities of NO without other stimuli, as early as 24 h postinfection. BMDCs from C3H mice produced significantly higher levels of NO than those from B6 mice ($P < 0.01$). The production of NO was inhibited by L-NMMA in BMDCs from both C3H and B6 mice. C3H BMDCs produced significantly more NO in response to the LPS stimulus than B6 counterparts. Interestingly, NO production by LPS-stimulated BMDCs from C3H mice, but not from B6 mice, was suppressed in the presence of rickettsiae.

Rickettsial infection induces BMDC maturation. We evaluated the effect of *R. conorii* infection on the maturation status of BMDCs. Uninfected BMDC cultures derived from naïve C3H and B6 mice contained approximately 70 to 85% immature CD11c+ BMDCs (data not shown), as evidenced by low expression of major histocompatibility complex (MHC) class II
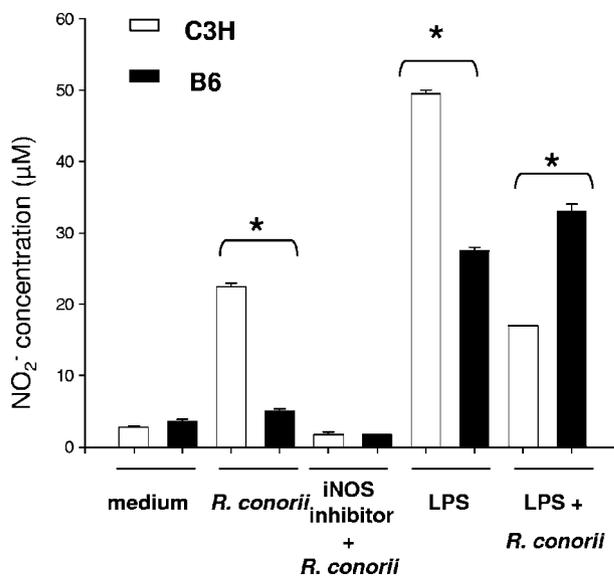

FIG. 3. NO induction by BMDCs following stimulation with *R. conorii* and LPS. BMDCs from C3H mice and B6 mice were left untreated or treated with *R. conorii* (MOI of 5), *R. conorii* plus L-NMMA (1 mM), LPS (100 ng/ml), or LPS plus *R. conorii*. After 24 h of stimulation, supernatants were collected for measurement of the concentration of NO_2^-. Data shown are representative of two independent experiments. *, $P < 0.01$.

B6

C3H
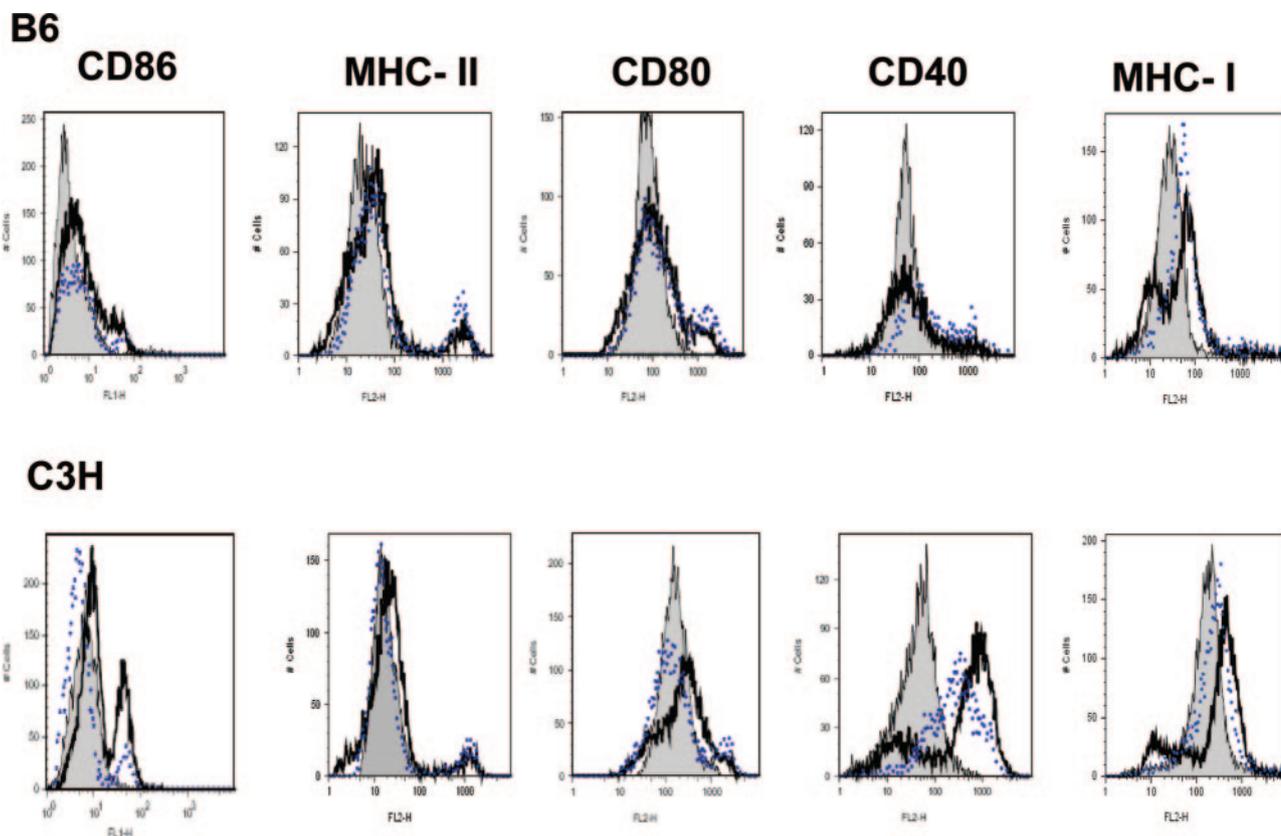
Mean Fluorescence Intensity (MFI) of BMDCs derived from resistant and susceptible mice

	CD86	MHC-II	CD80	CD40	MHC-I
B6 uninfected DCs	290	68	135	95	119
LPS-treated DCs	640	2518	478	688	278
R. conorii-infected DCs	777	2539	289	370	197
C3H uninfected DCs	110	125	598	58	380
LPS-treated DCs	465	1239	1267	458	482
R. conorii-infected DCs	735	1042	828	700	603

FIG. 4. BMDC maturation and activation following stimulation with *R. conorii* or LPS. BMDCs of B6 and C3H mice were left untreated (gray solid peaks) or stimulated with *R. conorii* strain Malish (black heavy lines) or LPS (blue dotted lines). After 24 h of stimulation, cells were stained with monoclonal Ab specific for CD11c and CD86, CD80, CD40, MHC-II, or MHC-I. Histograms depict expression profiles of gated CD11c$^+$ cells. Positive staining was determined based on staining profiles of isotype controls. Mean fluorescence intensities for each histogram are indicated in the table. Data are representative of three independent experiments with similar results.

and costimulatory molecules (Fig. 4). Stimulation of immature BMDCs from both mouse strains with LPS for 24 h resulted in their maturation as determined by higher expression levels of MHC class I, MHC class II, and costimulatory molecules such

as CD80, CD86, and CD40 (Fig. 4). *R. conorii* infection also resulted in BMDC maturation, as evidenced by significantly higher expression of MHC class II, MHC class I, CD40, CD86, and CD80 in both C3H and B6 mice compared to their unin-
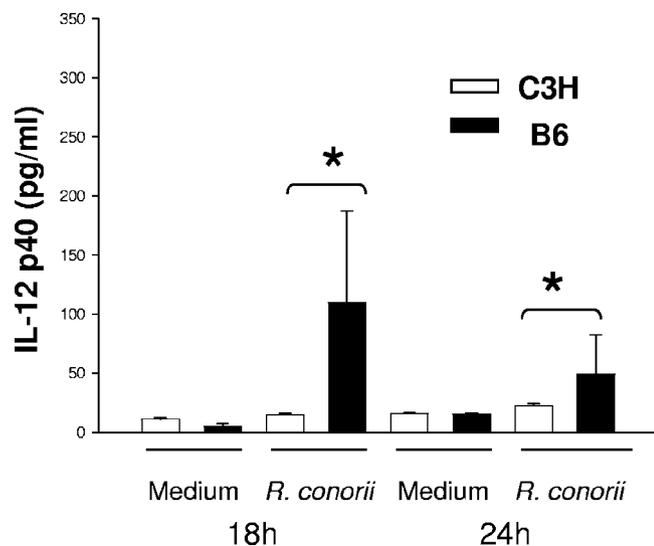
FIG. 5. IL-12p40 production by *R. conorii*-exposed BMDCs. BMDCs were derived from C3H mice and B6 mice and infected with *R. conorii*. Supernatants were collected at 18 h and 24 h postinfection. Cytokine production was examined by ELISA. Results are representative of two individual experiments with similar results. *, $P < 0.01$.

fected BMDCs (Fig. 4). The expression levels of these maturation markers by *R. conorii*-infected BMDCs were comparable to those by cells exposed to LPS. Although the rate of infection of BMDCs from both C3H and B6 mice was 100%, as described above (Fig. 1), the mean fluorescence intensity of MHC class II on *R. conorii*-infected BMDCs from B6 and C3H mice was 30- and 8-fold higher than that of uninfected BMDCs from each mouse strain, respectively (Fig. 4). Compared to uninfected BMDCs, *Rickettsia*-infected C3H BMDCs exhibited greater upregulation of expression of CD40 (12-fold increase) than B6 mice (4-fold increase). These data showed that there were quantitative differences in BMDC maturation induced by rickettsial infection between resistant and susceptible mice.

Differential effects of *R. conorii* on cytokine production by C3H and B6 BMDCs. Activated DCs produce a variety of cytokines (e.g., IL-12 and IL-4) that polarize CD4$^+$ T-cell subset development (6, 35). Therefore, we examined whether BMDCs from susceptible C3H or resistant B6 mice produced different cytokine profiles, which might contribute to a distinct Th cell response. Compared to uninfected cells, *R. conorii*-infected BMDCs derived from B6 mice produced significantly higher levels of IL-12p40 at 18 h and 24 h postinfection than C3H mice (Fig. 5). Maximal IL-12p40 production by B6 BMDCs was observed as early as 18 h after in vitro rickettsial infection and declined progressively thereafter (Fig. 5). Despite evident IL-12p40 production, little of the bioactive form of IL-12, IL-12p70, was detected when BMDCs of both mouse strains were infected with *R. conorii*. In comparison with negative controls, BMDCs from neither C3H nor B6 mice produced a significant quantity of IL-4 at 18 h and 24 h postrickettsial infection (data not shown). IFN-γ was not detected in *Rickettsia*-infected B6 or C3H BMDCs under the culture conditions examined. Taken together, our data suggest that rickettsial infection of BMDCs from resistant B6 mice, but not

susceptible C3H mice, resulted in a completely mature phenotype of BMDCs as judged by IL-12p40 production.

Differential naïve CD4$^+$ T-cell activation and proliferation patterns in resistant versus susceptible mice in vitro. To determine whether rickettsiae-infected BMDCs from C3H and B6 mice stimulate activation of naïve syngeneic CD4$^+$ T cells, T cells were analyzed for expression of the early activation marker CD69 at different time intervals following DC–T-cell coculture in vitro. Rickettsiae-infected BMDCs from B6 mice rapidly and substantially stimulated naïve syngeneic CD4$^+$ T cells to express CD69, whereas rickettsiae-infected BMDCs from C3H mice had a delayed effect on T-cell activation (Fig. 6A). At 72 h, CD4$^+$ T cells from resistant mice comprised two major populations with different cell sizes, granularity, and levels of CD69 expression (CD69^{high} and CD69^{low}) (Fig. 6B). In contrast, only one cell population of CD69-expressing CD4$^+$ T cells was observed in the DC–T-cell coculture from C3H mice. To determine whether differential T-cell activation levels in resistant mice would result in differential T-cell function, we measured early IFN-γ production by CD4$^+$ T cells. Our data showed that CD69^{low} CD4$^+$ T cells exhibited greater IFN-γ expression than CD69^{high} CD4$^+$ T cells following coculture with *R. conorii*-infected BMDCs for 72 h (Fig. 6B).

Differential differentiation of naïve CD4$^+$ T cells of C3H versus B6 mice promoted by *R. conorii*-infected BMDCs in vitro. To determine the effects of *Rickettsia*-infected BMDCs on Th1 and Th2 differentiation of naïve syngeneic CD4$^+$ T cells, we further cocultured CD4$^+$ T cells with uninfected immature BMDCs, mature BMDCs infected with *R. conorii*, or mature BMDCs activated with LPS. After 5 days of coculture in the presence of IL-2, we analyzed IFN-γ- or IL-4-secreting CD4$^+$ CD3$^+$ T cells by flow cytometry. As shown in Fig. 7A, LPS-activated BMDCs from B6 mice induced syngeneic CD4$^+$ T-cell differentiation into a Th1 phenotype, while LPS-activated BMDCs from C3H mice stimulated a mixed Th1/Th2 phenotype of syngeneic CD4$^+$ T cells. Interestingly, *R. conorii*-infected BMDCs from B6 mice polarized syngeneic CD4$^+$ T cells into a predominant Th1 immune response similar to LPS-activated BMDCs, where the number of *Rickettsia*-dependent IFN-γ-producing CD4$^+$ Th1 cells was significantly higher than *Rickettsia*-dependent IL-4-producing CD4$^+$ T cells (Fig. 7A). In contrast, *R. conorii*-infected BMDCs from C3H mice suppressed both IFN-γ- and IL-4-expressing T cells compared to either uninfected BMDCs or LPS-activated BMDCs (Fig. 7A). Similarly, analysis of antigen-dependent IFN-γ and IL-4 production by ELISA indicated that *R. conorii*-infected BMDCs and LPS-activated BMDCs from B6 mice promoted a Th1 response. Interestingly, in the DC–T-cell coculture system from C3H mice, compared to LPS-activated BMDCs that promoted a Th2 response, *R. conorii*-infected BMDCs induced Th1 cytokine production (Fig. 7B). No significant difference in the concentration of antigen-dependent IL-10 was detected in the supernatant of CD4$^+$ T cells derived from C3H or B6 mice cocultured with either *R. conorii*-infected or LPS-activated BMDCs.

Induction of CD4$^+$ CD25$^+$ Foxp3$^+$ T regulatory cells in vitro by *R. conorii*-infected BMDCs from susceptible and resistant mice. Because the above in vitro data suggested antigen-dependent suppression of CD4$^+$ T-cell responsiveness upon coculture with *R. conorii*-infected C3H BMDCs, we next
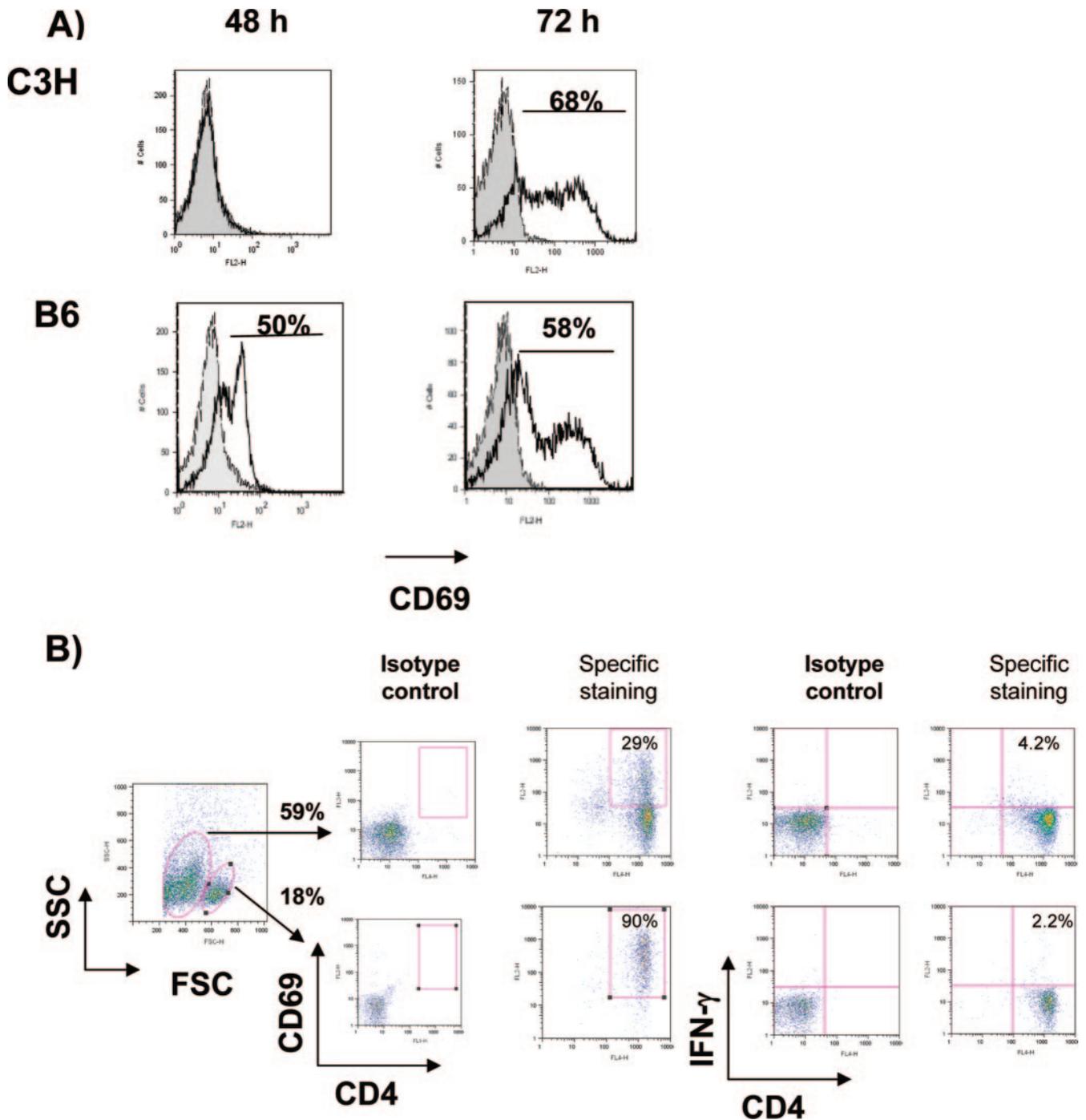
FIG. 6. Activation of naïve T cells by *R. conorii*-infected BMDCs. BMDCs of B6 and C3H mice were infected with *R. conorii* and then cocultured with naïve syngeneic CD4$^+$ T cells as described in Materials and Methods. (A) At 48 and 72 h of coculture, CD4$^+$ CD3$^+$ T cells were analyzed for surface expression of CD69. Isotype controls are shown in solid gray, and CD4$^+$ T cells activated by infected BMDCs are shown as black lines. (B) At 72 h of coculture, the percentages of CD69-expressing- and IFN-γ-producing CD4$^+$ CD3$^+$ T cells from B6 mice were determined among the two cell populations that were identified according to differences in cell size and granularity. Data are representative of two independent experiments.

determined whether *R. conorii*-infected C3H BMDCs promoted the expansion of T regulatory cells. We found that in the absence of antigen but the presence of IL-2, uninfected BMDCs stimulated the expansion of CD4$^+$ Foxp3$^+$ regulatory T cells in both C3H and B6 groups (Fig. 8). These data were

consistent with prior studies showing that immature BMDCs initiate strong T regulatory cell activity in the absence of any exogenous stimulus (15, 18). The frequencies of CD4$^+$ Foxp3$^+$ regulatory T cells were markedly reduced to 15% in LPS-activated B6 BMDCs in comparison to their controls (38%).
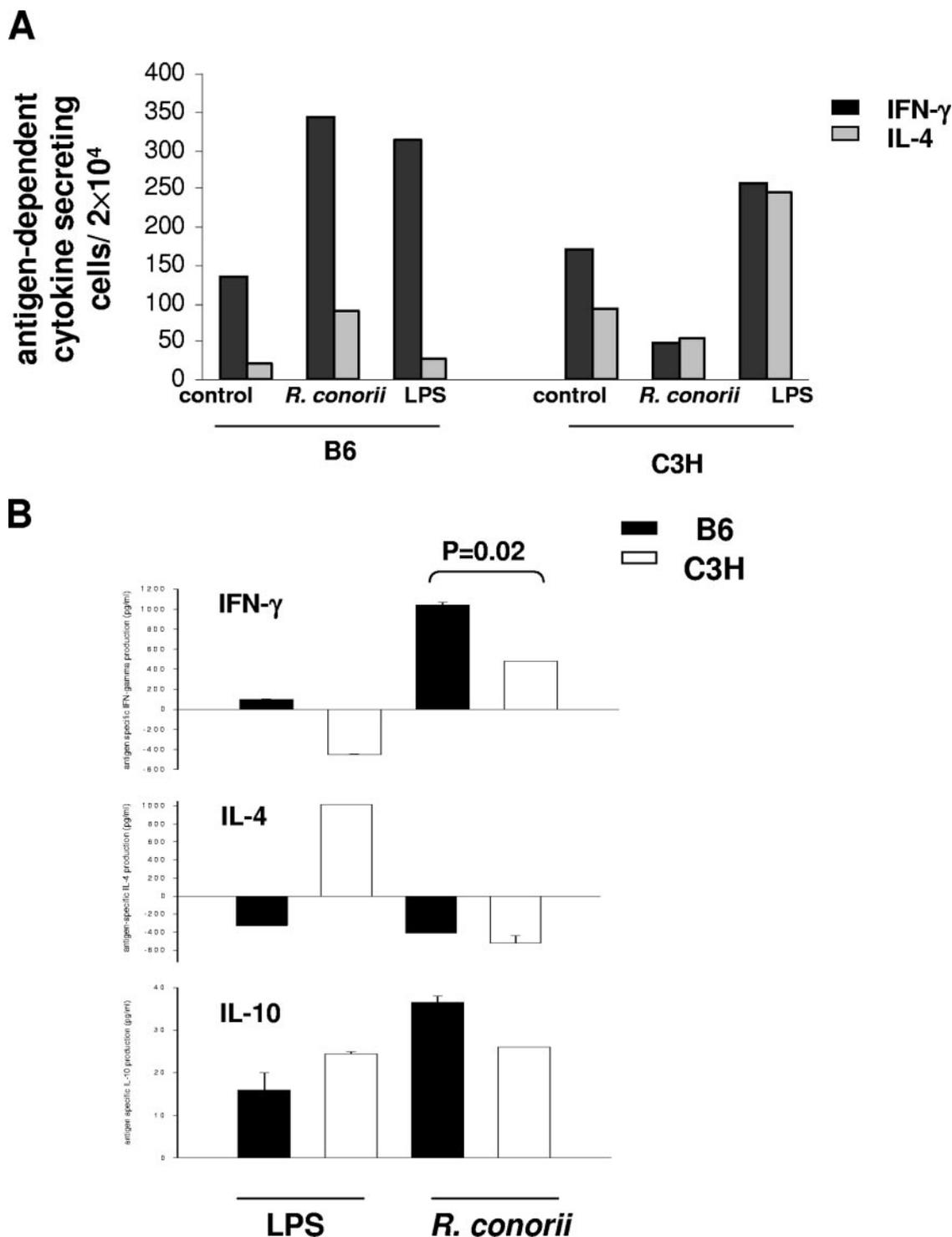
A

B

FIG. 7. In vitro priming of naïve syngeneic CD4+ T cells by *R. conorii*-infected BMDCs. BMDCs of C3H and B6 mice were infected with *R. conorii* and cocultured with naïve syngeneic CD4+ T cells as described in Materials and Methods. (A) On day 5 of coculture, the frequencies of IFN-γ- and IL-4-producing CD3+ CD4+ T cells were analyzed by flow cytometry. (B) The levels (in pg/ml) of antigen-dependent cytokine induction in culture supernatants were assayed by ELISA. Antigen-dependent or LPS- induced cytokine induction was considered as the level of cytokine detected in coculture of T cells with *R. conorii*-infected or LPS-treated BMDCs, from which was subtracted the level of the same cytokine in coculture of T cells incubated with uninfected BMDCs. Samples were performed in triplicate. Data are representative of two independent experiments.
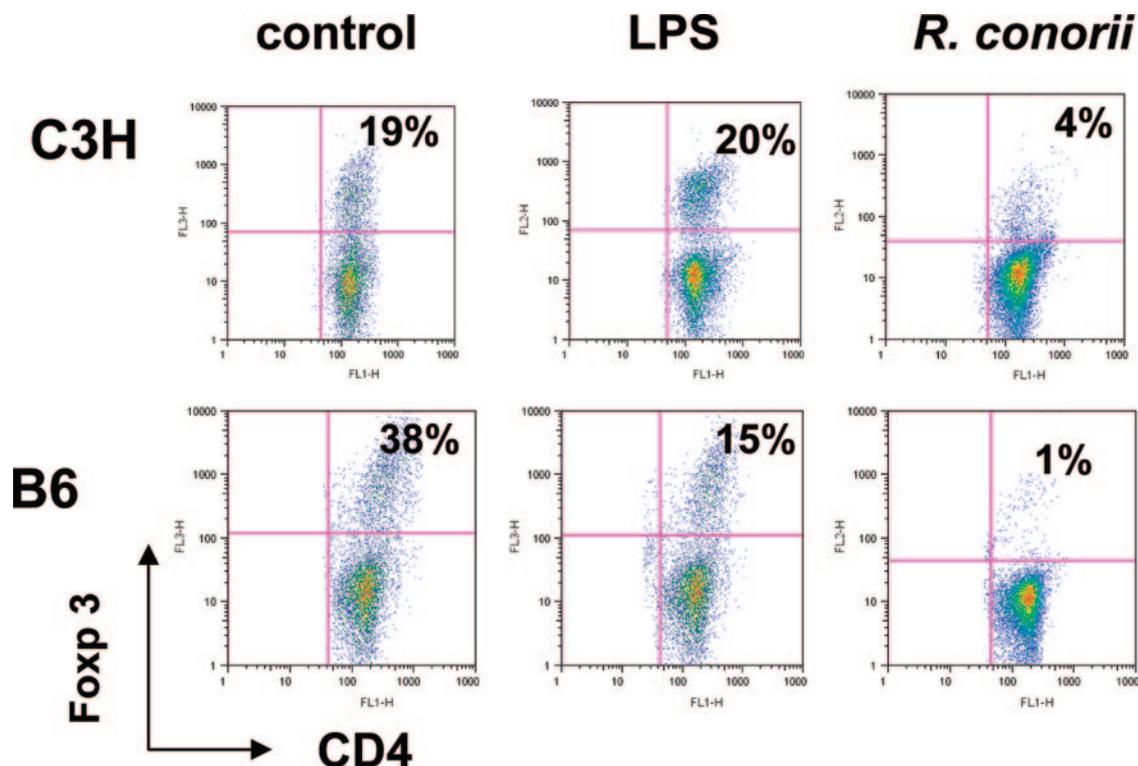
FIG. 8. Frequencies of regulatory T cells induced by syngeneic *R. conorii*-infected BMDCs in vitro. BMDCs of C3H and B6 mice were left untreated or stimulated with *R. conorii* or LPS as described for Fig. 7. After washing, BMDCs were cocultured with naïve syngeneic CD4$^+$ cells for 5 days. The frequencies of Foxp3$^+$ CD4$^+$ T cells were analyzed by flow cytometry. Cells were gated only on CD3$^+$ T cells. For each sample, 20,000 events were collected. Results are representative of two independent experiments.

This type of reduction, however, was not observed in C3H BMDCs (19% in T cells cocultured with uninfected BMDCs versus 20% in T cells cocultured with LPS-activated BMDCs). Interestingly, *R. conorii*-infected BMDCs initiated decreased frequencies of Foxp3$^+$ syngeneic T regulatory cells following DC–T-cell coculture in both C3H and B6 groups. However, we found 38-fold and 5-fold reductions in the frequencies of syngeneic Foxp3$^+$ T regulatory cells following coculture with *R. conorii*-infected B6 and C3H BMDCs, respectively, compared to those cocultured with uninfected BMDCs (Fig. 8). Thus, *Rickettsia*-activated, mature BMDCs from susceptible and resistant backgrounds differ in their capacity to stimulate the expansion of regulatory CD4$^+$ T cells in vitro.

DISCUSSION

In this study, we characterized for the first time the interactions of BMDCs from mice that are resistant and susceptible to spotted fever rickettsiosis, which initiated differential T helper cell responses in vitro. Our results suggest that *R. conorii*-infected BMDCs from resistant mice possess higher phagocytic and bactericidal capacities and exhibit a full maturation status marked by higher levels of MHC class II as well as a greater IL-12p40 production than BMDCs from susceptible mice. In vitro results of DC–T-cell coculture suggested that *R. conorii*-infected BMDCs from resistant B6 mice supported the development of CD4$^+$ Th1 cells while infected BMDCs from susceptible C3H mice promoted the expansion of T regulatory

cells, which might explain host susceptibility to fatal rickettsiosis.

In this report, BMDCs from both C3H and B6 mice had a 100% infection rate at 24 h postinfection with rickettsiae (data not shown). This infection rate is higher than that reported for other intracellular pathogens, such as *Leishmania major*, where amastigotes infect only 36% of fetal skin-derived DCs at 18 h after inoculation (45). Unlike professional phagocytes, the major function of DCs is not to clear pathogens but to present antigens to the immune system (37). Quantification of intracellular rickettsiae in BMDCs (Fig. 2) suggested that B6 BMDCs captured and sampled rickettsial antigen with a higher efficiency than those in susceptible mice, which correlates with increased expression of MHC class II (Fig. 4). Bottomly and colleagues have shown that critical factors, including the antigen dose and the density of T-cell receptor ligands (i.e., signal one), skewed Th1/Th2 responses (5). Therefore, it is most likely that the higher antigen uptake by BMDCs from B6 mice results in abundance of rickettsiae-derived peptides bound to a greater number of MHC class II molecules, which in turn provide strong T-cell receptor signals to naïve CD4$^+$ T cells, promoting their differentiation into the Th1 phenotype. This notion might explain our observations of increased MHC class II expression on infected B6 BMDCs (Fig. 4) and a Th1-dominant immune response in DC–T-cell coculture from B6 mice (Fig. 7).

Early escape from the phagosomal vacuole is essential for growth and virulence of some intracellular pathogens. *Rick-*

ettsia enters other host cells in membrane-bound vacuoles (phagosomes), but it escapes into the cytosol in a short time (~5 to 10 min) (Fig. 1A). Our ultrastructural studies suggested that rickettsiae were effectively internalized by BMDCs from both B6 and C3H mice. Interestingly, unlike cytoplasmic localization within endothelial target cells, rickettsiae localized within vacuoles as well as in the cytosol of infected BMDCs from mice of both genetic backgrounds. The presence of rickettsiae in both vacuoles and cytosol in BMDCs may enhance their T-cell priming function through their ability to present rickettsial antigens residing in phagosomes and cytosol through MHC class II and I pathways, respectively, to CD4$^+$ and CD8$^+$ T cells.

Rickettsial infection of BMDCs from both mouse strains results in BMDC maturation as characterized by upregulated MHC class I and II molecules, as well as costimulatory molecules, including CD80, CD86, and CD40 (Fig. 4). However, our data show quantitative differences in expression levels of maturation markers between C3H and B6 BMDCs, which could be due to different stages of maturation (Fig. 4). Specifically, *Rickettsia*-infected BMDCs from resistant B6 mice expressed a higher amount of MHC class II but lower levels of CD40 molecules compared to *Rickettsia*-infected BMDCs from C3H mice (Fig. 4). Previous studies have demonstrated that expression of CD40 on DCs correlates closely with a Th2-type immune response (23, 32). Although we did not detect a Th2 response in T-cell cocultures with BMDCs from either C3H or B6 mice, we observed a suppressed syngeneic CD4$^+$ T-cell response stimulated by *R. conorii*-infected C3H BMDCs that substantially upregulated their CD40 expression (12-fold increase compared to uninfected controls, as shown in Fig. 4). It remains to be determined if CD40-CD40L interactions are associated with a suppressive T-cell response. On the other hand, it is possible that an intermediate (fourfold increase compared to uninfected controls), but optimal, upregulation of CD40 expression on B6 BMDCs was responsible for their ability to skew CD4$^+$ T cells towards a Th1 phenotype that was observed in DC–T-cell cocultures in vitro (Fig. 7).

The dichotomy of type 1 and type 2 cells stands as a central paradigm that provides the framework to understand the nature of an immune response that is either beneficial or detrimental to the host (34, 52). Our data showed that uptake of a larger number of *R. conorii* correlated with a higher level of IL-12p40 production in B6 BMDCs compared to those of C3H counterparts (Fig. 5). The production of IL-12p40 by B6 BMDCs was linked to their ability to induce early activation of naïve syngeneic CD4$^+$ T cells and their differentiation into a Th1 phenotype (Fig. 6 and 7A). Several studies have shown that antigen-presenting cell-derived IL-12 plays a definitive role in the development of Th1 responses (5, 16, 38, 40, 41). IL-12p40 is a common subunit of IL-12p70 and IL-23, which are both bioactive Th1 cytokines (43). Although we did not detect any IL-12p70 production in in vitro BMDCs cultures of either mouse strain, this does not exclude the possibility that biologically active IL-12p70 may be produced in vivo by *Rickettsia*-infected BMDCs. In similar BMDC in vitro cultures from C3H mice, the presence or absence of IL-12p40 showed a close correlation with the presence or absence of IL-23 (25). Whether IL-23 is produced by infected BMDCs from C3H and B6 mice both in vitro and in vivo is worth investigating. Nevertheless, our studies suggest that IL-12p40 production by B6 BMDCs could account for the observed Th1-dominant response in resistant mice as shown by DC–T-cell coculture in vitro (Fig. 7A). The inability of *Rickettsia*-infected BMDCs from C3H mice to produce a significant level of IL-12p40 is not due to an inhibitory effect of Th2 cytokines such as IL-4, as we did not detect significant levels of these cytokines in our in vitro BMDC cultures (data not shown). It has been reported that IL-12p40 production by DCs correlates closely with high bacterial burdens, DC maturation status, different Toll-like receptor (TLR) activity, and different phenotype subsets (5, 26, 27, 30, 42). Our data do not support the possibility that high IL-12p40 production by B6 BMDCs is due to a different DC phenotype subset, since BMDCs from both mice strains were of the CD11c$^+$ CD11b$^+$ CD8α$^-$ phenotype as determined by flow cytometry (data not shown). Thus, our data suggest that production of IL-12p40 in resistant mice could be due to a higher bacterial burden (Fig. 2) and/or to a different maturation status (Fig. 4).

Our study also provides evidence that NO plays a role in microbicidal effector functions of DCs of both mouse strains. The ability of B6 BMDCs to control intracellular bacterial replication (Fig. 2 and 3) in the presence of a lower level of NO compared to infected C3H BMDCs suggests that in vitro microbicidal activity of B6 BMDCs is mediated by both NO-dependent and NO-independent mechanisms. On the other hand, compared to B6 BMDCs, the higher amount of NO produced by infected C3H BMDCs suggested that their in vitro microbicidal activities were predominantly mediated by NO. We and others have demonstrated that different microbicidal mechanisms are involved in elimination of rickettsiae or other related organisms, such as *Ehrlichia*, within different target cells (11, 36). These mechanisms may include phagosome-lysosome fusion, tryptophan degradation, reactive oxygen species, NO, and limitation of iron availability and warrant further investigation. Interestingly, we found that rickettsiae inhibit NO production by LPS-stimulated C3H BMDCs but not B6 BMDCs (Fig. 3). While the mechanisms underlying this inhibition remain unclear, it has been suggested that differences in cytokines such as IL-10 and TLR signaling could mediate differential NO production by different cell types (29, 49). It is possible that inhibition of NO production is mediated by soluble suppressor cytokines such as IL-10. Furthermore, ligation of different TLRs on LPS-stimulated DCs by rickettsiae could also account for the observed NO inhibition. These possibilities are currently under our investigation.

Finally, our data show that *Rickettsia*-infected BMDCs from resistant B6 mice induced early activation of naïve CD4$^+$ T cells and differentiation into IFN-γ-producing Th1 cells, while *Rickettsia*-infected BMDCs from susceptible C3H mice induced late CD4$^+$ T-cell activation and suppressed Th1 and Th2 responses (Fig. 6 and 7). Three potential mechanisms were involved in late T-cell activation in C3H mice compared to B6 mice in vitro. (i) At 24 h postinfection, BMDCs might have been deficient in providing a second signal for T-cell activation, such as CD80, CD86, and CD40, which is not supported by the current results (Fig. 4). (ii) Recently, West et al. demonstrated that persistent CD80/CD86 signaling during prolonged interactions with DCs allows naïve T cells to express CD69 and enter the cell cycle (28). In vitro-infected C3H

BMDCs might have defects in prolonged or persistent expression of higher amounts of costimulatory molecules from 24 h to 48 h postinfection, which could result in the late CD69 expression on T cells. (iii) It is also possible that differences in the first signal (MHC class I and II and antigen presentation) rather than the second signal accounts for differential T-cell activation between B6 mice and C3H mice. Our data support this possibility, as evidenced by higher MHC class II levels on infected B6 BMDCs (Fig. 4), higher internalization of rickettsiae (Fig. 2A, 4-h time point), and prolonged antigen presentation as evidenced by more effective control of intracellular rickettsiae in B6 BMDCs at 48 h postinfection than in C3H BMDCs (Fig. 2C). Interestingly, at 72 h after coculture of naïve $CD4^+$ T cells with *R. conorii*-infected B6 BMDCs, but not C3H BMDCs, we detected two populations of $CD4^+$ T cells with different levels of CD69 ($CD69^{low}$ and $CD69^{high}$) and IFN-γ expression (Fig. 6). Recent studies have shown that expression of CD69 occurs soon after activation, at a stage preceding cell division, and then the expression progressively declines with increasing IFN-γ production (3, 14). Therefore, the higher production of IFN-γ by $CD69^{low}$ $CD4^+$ T cells and vice versa might reflect different stages of cell division. Although our analysis of in vitro responsiveness of $CD4^+$ T cells detected a heterogeneous population, it is unlikely that the $CD69^{low}$ and $CD69^{high}$ $CD4^+$ T cells represent a mixture of effector $CD4^+$ $CD25^-$ T cells and $CD4^+$ $CD25^+$ T regulatory cells with a different activation status, since regulatory T cells are known to be defective in IFN-γ production.

Immature and mature DCs are important cells in regulating $CD25^+$ $CD4^+$ T regulatory cell function and expansion, although little is known about the manner by which this may occur (2, 8, 15, 33). We detected expansion of $Foxp3^+$ T regulatory cells among T cells cocultured with uninfected BMDCs in both C3H and B6 mice. These data are consistent with other studies suggesting that self antigens expressed by immature DCs play a role in the induction of T regulatory cells, which was hypothesized to be a mechanism of maintaining normal immunohomeostasis in vivo (15). Compared to the frequencies of T regulatory cells induced by uninfected BMDCs in vitro, *R. conorii*-infected B6 BMDCs showed strikingly less expansion of T regulatory cells than C3H BMDCs (Fig. 8). Naturally occurring $CD4^+$ $CD25^+$ $Foxp3^+$ regulatory T cells are critical for the prevention of autoimmunity but can also hamper effective control of microbial infections (18). Thus, the greater frequency of T regulatory cells correlates with greater downregulation of effector $CD4^+$ $CD25^-$ T cells and the more-suppressive T-cell response. This may be the case in our study, where a less-reduced expansion of T regulatory cells in DC–T-cell coculture from susceptible C3H mice was associated with lower frequencies of both Th1 and Th2 cells compared to B6 mice (Fig. 7A). Importantly, this observation in C3H mice in vitro correlates well with the previous in vivo study, which suggests that a transient immunosuppressive response was induced in this murine model of endothelial target rickettsiosis (47). However, the mechanisms by which T regulatory cells may mediate suppression in *R. conorii*-infected C3H mice remain to be resolved. Analysis of Th1/Th2 responses by ELISA demonstrated IFN-γ production in C3H DC–T-cell culture supernatant. Since we observed suppressed $CD4^+$ Th1 and Th2 responses by flow cytometry in the same coculture system,

the presence of IFN-γ in DC–T-cell coculture supernatant was likely derived from BMDCs activated upon their interaction with activated $CD4^+$ T cells.

In summary, our study provided the first evidence that differential interactions of rickettsiae with BMDCs might greatly contribute to different host susceptibilities to rickettsial diseases. Our in vitro DC–T-cell coculture allows the analysis of the DC–T-cell interaction upon rickettsial infection without confounding problems in interpretation due to multiple cellular interactions that exist in vivo. Our study suggests that interactions of rickettsiae with DCs at the early stages of infection may determine the differential severity of rickettsial disease, presumably by supporting the development of either protective Th1 cells or suppressive and detrimental $CD4^+$ T regulatory cells in resistant or susceptible hosts, respectively.

REFERENCES

1. **Amaro, M., F. Bacellar, and A. Franca.** 2003. Report of eight cases of fatal and severe Mediterranean spotted fever in Portugal. Ann. N. Y. Acad. Sci. **990:**331–343.
2. **Banchereau, J., F. Briere, C. Caux, J. Davoust, S. Lebecque, Y.-J. Liu, B. Pulendran, and K. Palucka.** 2000. Immunobiology of dendritic cells. Annu. Rev. Immunol. **18:**767–811.
3. **Bird, J. J., D. R. Brown, A. C. Mullen, N. H. Moskowitz, M. A. Mahowald, J. R. Sider, T. F Gajewski, C. R. Wang, and S. L. Reiner.** 1998. Helper T cell differentiation is controlled by the cell cycle. Immunity **9:**229–237.
4. **Brzoza, K. L., A. B. Rockel, and E. M. Hiltbold.** 2004. Cytoplasmic entry of *Listeria monocytogenes* enhances dendritic cell maturation and T cell differentiation and function. J. Immunol. **173:**2641–2651.
5. **Constant, S. L., and K. Bottomly.** 1997. Induction of Th1 and Th2 $CD4^+$ T cell responses: the alternative approaches. Annu. Rev. Immunol. **15:**297–322.
6. **de Saint-Vis, B., I. Fugier-Vivier, C. Massacrier, C. Gaillard, B. Vanbervliet, S. it-Yahia, J. Banchereau, Y. J. Liu, S. Lebecque, and C. Caux.** 1998. The cytokine profile expressed by human dendritic cells is dependent on cell subtype and mode of activation. J. Immunol. **160:**1666–1676.
7. **de Sousa, R., S. D. Nobrega, F. Bacellar, and J. Torgal.** 2003. Mediterranean spotted fever in Portugal: risk factors for fatal outcome in 105 hospitalized patients. Ann. N. Y. Acad. Sci. **990:**285–294.
8. **Fehervari, Z., and S. Sakaguchi.** 2004. Control of $Foxp3^+$ $CD25^+$ $CD4^+$ regulatory cell activation and function by dendritic cells. Int. Immunol. **16:**1769–1780.
9. **Feng, H. M., V. L. Popov, and D. H. Walker.** 1994. Depletion of gamma interferon and tumor necrosis factor alpha in mice with *Rickettsia conorii*-infected endothelium: impairment of rickettsicidal nitric oxide production resulting in fatal, overwhelming rickettsial disease. Infect. Immun. **62:**1952–1960.
10. **Feng, H. M., and D. H. Walker.** 1993. Interferon-gamma and tumor necrosis factor-alpha exert their antirickettsial effect via induction of synthesis of nitric oxide. Am. J. Pathol. **143:**1016–1023.
11. **Feng, H. M., and D. H. Walker.** 2000. Mechanisms of intracellular killing of *Rickettsia conorii* in infected human endothelial cells, hepatocytes, and macrophages. Infect. Immun. **68:**6729–6736.
12. **Feng, H. M., J. Wen, and D. H. Walker.** 1993. *Rickettsia australis* infection: a murine model of a highly invasive vasculopathic rickettsiosis. Am. J. Pathol. **142:**1471–1482.
13. **Feng, H. M., T. Whitworth, V. L. Popov, and D. H. Walker.** 2004. Effect of antibody on the rickettsia-host cell interaction. Infect. Immun. **72:**3524–3530.
14. **Fulcher, D., and S. Wong.** 1999. Carboxyfluorescein succinimidyl ester-based proliferative assays for assessment of T cell function in the diagnostic laboratory. Immunol. Cell Biol. **77:**559–564.
15. **Gad, M., N. N. Kristensen, E. Kury, and M. H. Claesson.** 2004. Characterization of T-regulatory cells, induced by immature dendritic cells, which inhibit enteroantigen-reactive colitis-inducing T-cell responses in vitro and in vivo. Immunology **113:**499–508.
16. **Gorak, P. M., C. R. Engwerda, and P. M. Kaye.** 1998. Dendritic cells, but not macrophages, produce IL-12 immediately following *Leishmania donovani* infection. Eur. J. Immunol. **28:**687–695.
17. **Hanson, B. A., C. L. Wisseman, Jr., A. Waddell, and D. J. Silverman.** 1981. Some characteristics of heavy and light bands of *Rickettsia prowazekii* on renografin gradients. Infect. Immun. **34:**596–604.

18. **Hori, S., T. L. Carvalho, and J. Demengeot.** 2002. CD25$^+$ CD4$^+$ regulatory T cells suppress CD4$^+$ T cell-mediated pulmonary hyperinflammation driven by *Pneumocystis carinii* in immunodeficient mice. Eur. J. Immunol. **32:**1282–1291.

19. **Inaba, K., M. Inaba, N. Romani, H. Aya, M. Deguchi, S. Ikehara, S. Muramatsu, and R. M. Steinman.** 1992. Generation of large numbers of dendritic cells from mouse bone marrow cultures supplemented with granulocyte/macrophage colony-stimulating factor. J. Exp. Med. **176:**1693–1702.

20. **Ingulli, E., A. Mondino, A. Khoruts, and M. K. Jenkins.** 1997. *In vivo* detection of dendritic cells antigen presentation to CD4$^+$ T cells. J. Exp. Med. **185:**2133–2141.

21. **Ismail, N., J. P. Olano, H. M. Feng, and D. H. Walker.** 2002. Current status of immune mechanisms of killing of intracellular microorganisms. FEMS Microbiol. Lett. **207:**111–120.

22. **Ito, S., and Y. Rikihisa.** 1981. Techniques for electron microscopy of rickettsiae, p. 213–227. *In* W. Burgdorfer and R. L. Anacker (ed.), Rickettsiae and rickettsial diseases. Academic Press, New York, NY.

23. **Jenkins, S. J., and A. P. Mountford.** 2005. Dendritic cells activated with products released by schistosome larvae drive Th2-type immune responses, which can be inhibited by manipulation of CD40 costimulation. Infect. Immun. **73:**395–402.

24. **Jonuleit, H., E. Schmitt, K. Steinbrink, and A. H. Enk.** 2001. Dendritic cells as a tool to induce anergic and regulatory T cells. Trends Immunol. **22:**394–400.

25. **Jordan, J. M., M. E. Woods, H. M. Feng, L. Soong, and D. H. Walker.** *Rickettsia*-stimulated dendritic cells mediate protection against lethal rickettsial challenge in an animal model of spotted fever rickettsiosis. J. Infect. Dis., in press.

26. **Kaisho, T., and S. Akira.** 2001. Dendritic-cell function in Toll-like receptor- and MyD88-knockout mice. Trends Immunol. **22:**78–83.

27. **Kaisho, T., and S. Akira.** 2001. Endotoxin-induced maturation of MyD88-deficient dendritic cells. J. Immunol. **166:**5688–5694.

28. **Kaisho, T., O. Takeuchi, T. Kawai, K. Hoshino, and S. Akira.** 2006. Prolonged costimulation is required for naive T cell activation. Immunol. Lett. **106:**135–143.

29. **Liew, F. Y., X. Q. Wei, and L. Proudfoot.** 1997. Cytokines and nitric oxide as effector molecules against parasitic infections. Philos. Trans. R. Soc. Lond. B **352:**1311–1315.

30. **Liu, T., T. Matsuguchi, N. Tsuboi, T. Yajima, and Y. Yoshikai.** 2002. Differences in expression of toll-like receptors and their reactivities in dendritic cells in BALB/c and C57BL/6 mice. Infect. Immun. **72:**6638–6645.

31. **Lutz, M. B., N. Kukutsch, A. L. Ogilvie, S. Rossner, F. Koch, N. Romani, and G. Schuler.** 1999. An advanced culture method for generating large quantities of highly pure dendritic cells from mouse bone marrow. J Immunol. Methods **223:**77–92.

32. **MacDonald, A. S., A. D. Straw, N. M. Dalton, and E. J. Pearce.** 2002. Cutting edge: Th2 response induction by dendritic cells: a role for CD40. J. Immunol. **168:**537–540.

33. **Mahnke, K., E. Schmitt, L. Bonifaz, A. H. Enk, and H. Jonuleit.** 2002. Immature, but not inactive: the tolerogenic function of immature dendritic cells. Immunol. Cell Biol. **80:**477–483.

34. **Mikhalkevich, N., B. Becknell, M. A. Caligiuri, M. D. Bates, R. Harvey, and W. P. Zheng.** 2006. Responsiveness of naive CD4 T cells to polarizing cytokine determines the ratio of Th1 and Th2 cell differentiation. J. Immunol. **176:**1553–1560.

35. **Moser, M., and K. M. Murphy.** 2000. Dendritic cell regulation of Th1-Th2 development. Nat. Immunol. **1:**199–205.

36. **Mott, J., and Y. Rikihisa.** 2000. Human granulocytic ehrlichiosis agent inhibits superoxide anion generation by human neutrophils. Infect. Immun. **68:**6697–6703.

37. **Nagl, M., L. Kacani, B. Mullauer, E. M. Lemberger, H. Stoiber, G. M. Sprinzl, H. Schennach, and M. P. Dierich.** 2002. Phagocytosis and killing of bacteria by professional phagocytes and dendritic cells. Clin. Diagn. Lab. Immunol. **9:**1165–1168.

38. **O'Garra, A.** 1998. Cytokines induce the development of functionally heterogeneous T helper cell subsets. Immunity **8:**275–283.

39. **Qi, H., V. L. Popov, and L. Soong.** 2001. *Leishmania amazonensis*-dendritic cell interactions *in vitro* and the priming of parasite-specific CD4$^+$ T cells *in vivo*. J. Immunol. **167:**4534–4542.

40. **Reis e Sousa, C., S. Hieny, T. Scharton-Kersten, D. Jankovic, H. Charest, R. N. Germain, and A. Sher.** 1997. *In vivo* microbial stimulation induces rapid CD40 ligand-independent production of interleukin 12 by dendritic cells and their redistribution to T cell areas. J Exp. Med. **186:**1819–1829.

41. **Reis e Sousa, C.** 2006. Dendritic cells in a mature age. Nat. Rev. Immunol. **6:**476–483.

42. **Sato, M., K. Iwakabe, S. Kimura, and T. Nishimura.** 1999. Functional skewing of bone marrow-derived dendritic cells by Th1- or Th2-inducing cytokines. Immunol. Lett. **67:**63–68.

43. **Trinchieri, G., S. Pflanz, and R. A. Kastelein.** 2003. The IL-12 family of heterodimeric cytokines: new players in the regulation of T cell responses. Immunity **19:**641–644.

44. **Valbuena, G., W. Bradford, and D. H. Walker.** 2003. Expression analysis of the T-cell-targeting chemokines CXCL9 and CXCL10 in mice and humans with endothelial infections caused by rickettsiae of the spotted fever group. Am. J. Pathol. **163:**1357–1369.

45. **von Stebut, E., Y. Belkaid, B. V. Nguyen, M. Cushing, D. L. Sacks, and M. C. Udey.** 2000. *Leishmania major*-infected murine Langerhans cell-like dendritic cells from susceptible mice release IL-12 after infection and vaccinate against experimental cutaneous leishmaniasis. Eur. J. Immunol. **30:**3498–3506.

46. **Walker, D. H., J. P. Olano, and H. M. Feng.** 2001. Critical role of cytotoxic T lymphocytes in immune clearance of rickettsial infection. Infect. Immun. **69:**1841–1846.

47. **Walker, D. H., V. L. Popov, J. Wen, and H. M. Feng.** 1994. *Rickettsia conorii* infection of C3H/HeN mice. A model of endothelial-target rickettsiosis. Lab. Investig. **70:**358–368.

48. **Walker, D. H., G. A. Valbuena, and J. P. Olano.** 2003. Pathogenic mechanisms of diseases caused by *Rickettsia*. Ann. N. Y. Acad. Sci. **990:**1–11.

49. **Werling, D., J. C. Hope, C. J. Howard, and T. W. Jungi.** 2004. Differential production of cytokines, reactive oxygen and nitrogen by bovine macrophages and dendritic cells stimulated with Toll-like receptor agonists. Immunology **111:**41–52.

50. **Wick, M. J.** 2003. The role of dendritic cells in the immune response to *Salmonella*. Immunol. Lett. **85:**99–102.

51. **Wykes, M., A. Pombo, C. Jenkins, and G. G. MacPherson.** 1998. Dendritic cells interact directly with naïve B lymphocytes to transfer antigen and initiate class switching in a primary T-dependent response. J. Immunol. **161:**1313–1319.

52. **Yokoo, T., K. Takakuwa, I. Ooki, A. Kikuchi, M. Tamura, and K. Tanaka.** 2006. Alteration of TH1 and TH2 cells by intracellular cytokine detection in patients with unexplained recurrent abortion before and after immunotherapy with the husband's mononuclear cells. Fertil. Steril. **85:**1452–1458.

53. **Yu, X.-J., and D. H. Walker.** 2005. Family I. *Rickettsiaceae*, p. 96–116 *In* D. J. Brenner, N. R. Kreig, and J. T. Staley (ed), Bergey's manual of systematic bacteriology, 2nd ed., vol. 2. Springer Science+Business Media, Inc., New York, NY.

Editor: W. A. Petri, Jr.